

1 **Drill site selection for cosmogenic nuclide exposure dating of the bed of the**  
2 **Greenland Ice Sheet**

3  
4 Jason P. Briner<sup>1\*</sup>, Caleb K. Walcott<sup>1</sup>, Joerg M. Schaefer<sup>2</sup>, Nicolás E. Young<sup>2</sup>, Joseph A.  
5 MacGregor<sup>3</sup>, Kristin Poinar<sup>1</sup>, Benjamin A. Keisling<sup>2</sup>, Sridhar Anandakrishnan<sup>4</sup>, Mary R. Albert<sup>5</sup>,  
6 Tanner Kuhl<sup>6</sup> and Grant Boeckmann<sup>6</sup>

7  
8 *1 Department of Geology, University at Buffalo, Buffalo, NY, 14260 USA*

9 *2 Lamont-Doherty Earth Observatory, Columbia University, Palisades, NY, USA*

10 *3 Cryospheric Sciences Laboratory, NASA Goddard Space Flight Center, Greenbelt, Maryland,*  
11 *USA*

12 *4 Department of Geosciences, Penn State University, University Park, PA 16802, USA*

13 *5 U.S. Ice Drilling Program, Thayer School of Engineering, Dartmouth College, Hanover, NH, USA*  
14 *Ice Drilling Program*

15 *6 U.S. Ice Drilling Program, University of Wisconsin-Madison, Madison, WI, USA*

16  
17 *\*Corresponding author, jbriner@buffalo.edu*  
18  
19  
20  
21  
22  
23  
24  
25  
26  
27  
28  
29

Deleted: Where to Green  
Deleted: ? S  
Formatted: Font color: Text 1

32 **1. Abstract**

33 Direct observations of the size of the Greenland Ice Sheet during Quaternary interglaciations  
34 are sparse yet valuable for testing numerical models of ice sheet history and sea level  
35 contribution. Recent measurements of cosmogenic nuclides in bedrock from beneath the  
36 Greenland Ice Sheet collected during past deep drilling campaigns reveal that the ice sheet was  
37 significantly smaller, and perhaps largely absent, sometime during the past 1.1 million years.  
38 These discoveries from decades-old basal samples motivate new, targeted sampling for  
39 cosmogenic nuclide analysis beneath the ice sheet. Current drills available for retrieving bed  
40 material from the US Ice Drilling Program require <700 m ice thickness and a frozen bed, while  
41 quartz-bearing bedrock lithologies are required for measuring a large suite of cosmogenic  
42 nuclides. We find that these and other requirements yield only ~3.4% of the Greenland Ice  
43 Sheet bed as a suitable drilling target using presently available technology. Additional factors  
44 related to scientific questions of interest are which areas of the present ice sheet are the most  
45 sensitive to warming, where a retreating ice sheet would expose bare ground rather than leave  
46 a remnant ice cap, and which areas are most likely to remain frozen bedded throughout glacial  
47 cycles and thus best preserve cosmogenic nuclides? Here we identify locations beneath the  
48 Greenland Ice Sheet that are best suited for potential future drilling and analysis. These include  
49 sites bordering Inglefield Land in northwestern Greenland, near Victoria Fjord and Mylius-  
50 Erichsen Land in northern Greenland, and inland from the alpine topography along the ice  
51 margin in eastern and northeastern Greenland. [Results from cosmogenic nuclide analysis in  
52 new sub-ice bedrock cores from these areas would help to constrain dimensions of the  
53 Greenland Ice Sheet in the past.](#)

54  
55

56 **2. Introduction**

57 Recent observations reveal significant ice loss in Greenland and Antarctica, with the  
58 Greenland Ice Sheet (GrIS) presently contributing more to sea level rise than the Antarctic Ice  
59 Sheet (AIS) (Shepherd et al., 2018; Shepherd et al., 2020). The higher potential for portions of  
60 the AIS to collapse due to marine ice-sheet instability, however, leaves estimates of future sea

61 level rise highly uncertain (Scambos et al., 2017; DeConto et al., 2021; Edwards et al., 2021).  
62 Non-linearities in ice sheet response to climate change also apply to the GrIS, which has been  
63 simulated to disappear in as little as one millennium (Aschwanden et al., 2019). Estimated rates  
64 of GrIS loss this century under the current trajectory of greenhouse-gas emissions (Goelzer et  
65 al., 2020; Edwards et al., 2021) have been shown to exceed those under natural variability over  
66 the past 12,000 years (Briner et al., 2020).

67 Although present rates of ice sheet loss are exceptional and concerning, there are few  
68 direct constraints on GrIS and AIS response to similar warmth during past interglaciations of the  
69 Quaternary (e.g., deVernal and Hillaire-Marcel, 2008; Schaefer et al., 2016). Thus, knowledge of  
70 ice sheet response under past climates that are comparable to the climate of our near future  
71 remains limited. Proxy data from geological archives, such as sedimentological characteristics in  
72 adjacent seas, have been used to evaluate ice sheet history, although these provide indirect  
73 evidence only for past changes in ice-sheet size. A growing body of evidence from offshore  
74 Greenland documents overall ice sheet growth and its subsequent oscillatory configurations  
75 throughout the Pliocene and Quaternary (e.g., Bierman et al., 2016, Knutz et al., 2019).  
76 Paleooceanographic studies have made valuable inferences of climate conditions (e.g., de Vernal  
77 and Hillaire-Marcel, 2008; Cluett and Thomas, 2021) and ice sheet configuration (e.g., Reyes et  
78 al., 2014; Hatfield et al., 2016) during brief interglacials. Generating direct knowledge of past  
79 GrIS response to interglacial warmth has proven difficult with these approaches. Farfield sea  
80 level reconstructions help to constrain GrIS response during past interglaciations (e.g., Dyer et  
81 al., 2021), yet still benefit from direct observations from individual ice sheets. Ice sheet  
82 modeling has simulated a variety of ice sheet volumes and configurations during past  
83 interglaciations (e.g., Goelzer et al., 2016; Robinson et al., 2017; Plach et al., 2018; Sommers et  
84 al., 2021), indicating more geologic measurements of ice-sheet extent are needed to evaluate  
85 these results.

86 The age of ice in basal ice core sections has been used to constrain the GrIS  
87 configuration during marine isotope stage (MIS) 5e (129-116 ka) and thus validate numerical  
88 simulations of ice size and configuration during the last interglacial (Otto-Bleisner et al., 2006;  
89 Plach et al., 2018; Domingo et al., 2020). However, there is some uncertainty about the role

Deleted: For example, a

Deleted: , but g

92 that ice advection plays in bringing aged ice over a previously ice-free location. For example,  
93 Yau et al. (2016a) found that the best fitting models for matching their elevation and  
94 temperature reconstructions for NEEM and GISP2 did not have ice at NEEM during MIS 5e,  
95 implying that the MIS 5e ice recovered at NEEM today not only flowed laterally but re-advanced  
96 over a deglaciated landscape. This phenomenon can be observed directly at the modern ice-  
97 sheet margin today, where Pleistocene-age ice outcrops at the margin in western Greenland  
98 (e.g., Reeh et al. 2002; MacGregor et al. 2020) where there was no ice as recently as the middle  
99 Holocene (Briner et al., 2010). Thus, it is critical to obtain independent information about sub-  
100 ice bedrock exposure age because apparently the age/stratigraphy of the overlying ice does not  
101 necessarily provide a continuous constraint on ice-cover history.

Deleted: the

Deleted: age

102 Fortunately, a new frontier of science is emerging, aimed at generating direct  
103 constraints on former ice sheet size using information collected from the ice sheet bed.  
104 Schaefer et al. (2016) measured cosmogenic  $^{10}\text{Be}$  and  $^{26}\text{Al}$  in bedrock obtained below the GISP2  
105 ice core (Figure 1), equipped with updated procedures and vastly improved analytic sensitivity  
106 relative to an earlier attempt (Nishiizumi et al., 1996). Their measurements require the GrIS to  
107 have been absent at the GISP2 locality for 280 kyr of the past 1.4 Myr. Although alternative  
108 histories are possible, the results [lead to an important conclusion: an almost entirely absent ice](#)  
109 [sheet in Greenland within the last 1.1 Myr. Furthermore, these types of data directly constrain](#)  
110 [past ice-sheet configurations, unlike marine sediment records from adjacent seas that provide](#)  
111 [indirect evidence](#). More recently, Christ et al. (2021) measured cosmogenic  $^{10}\text{Be}$  and  $^{26}\text{Al}$  in re-  
112 discovered sub-ice sediments in the Camp Century ice core collected in the 1960s (Figure 1).  
113 They interpret their results to indicate that the landscape below Camp Century became ice free  
114 at least once in the last 1.0 Myr. While one might expect the GrIS flank site of Camp Century to  
115 become ice free during some interglacial periods (model simulations commonly show this;  
116 Plach et al., 2018; Sommers et al., 2021), the findings from beneath the summit of the GrIS  
117 were more unexpected because model simulations rarely show ice-free conditions there (Briner  
118 et al., 2017). Additionally, new approaches have been developed to solve for long-term ice  
119 sheet occupation and subglacial erosion histories from vertical profiles of cosmogenic nuclides  
120 measured in multiple meters of rock core (Balter-Kennedy et al., 2021). Performing such

Deleted: point to

Deleted: significant

Deleted: loss

Deleted: within the Quaternary, and likely

127 analyses on new multi-meter-long bedrock cores from beneath the GrIS will be key for  
128 deciphering GrIS history.

129       Cosmogenic-nuclide measurements from sub-ice bed material in Greenland already  
130 have been shown to place direct constraints on past ice sheet history, despite the study of only  
131 two cosmogenic isotopes ( $^{10}\text{Be}$  and  $^{26}\text{Al}$ ) in these samples thus far. Additionally, the recent  
132 results from the sub-GrIS environment, although derived using legacy material from sites not  
133 targeted for cosmogenic-nuclide measurements, have demonstrated the power of this  
134 approach. While drilling technology that allows quick access (i.e., in a single field season) to the  
135 bed below ice sheet summits is being developed for application in Antarctica (Goodge and  
136 Severinghaus, 2016; Goodge et al., 2021), there is no such drill – or plans for one – to operate in

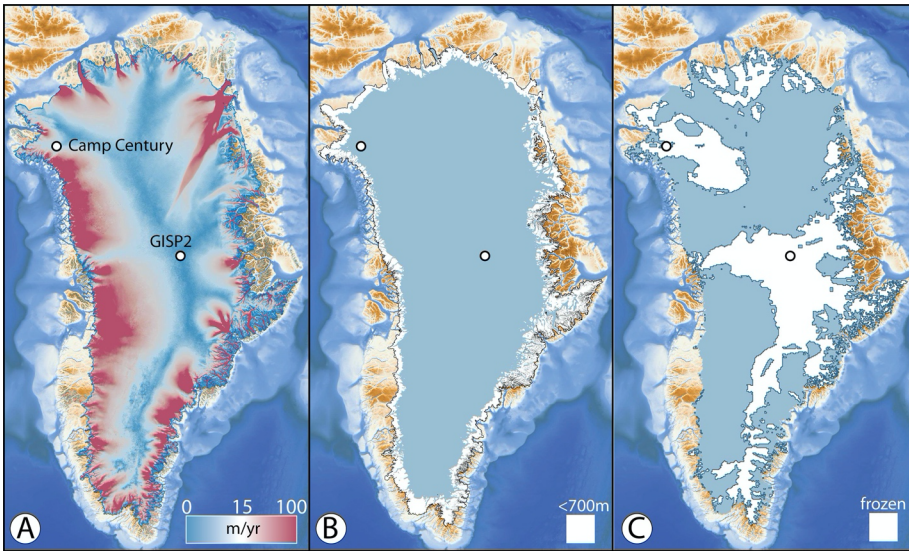


**Figure 1.** A. Horizontal surface velocities of the Greenland Sheet; the slowest flowing-areas define the summit ridge and ice divides; velocity from Greenland Ice Sheet velocity map from Sentinel-1, winter campaign 2019/2020 [version 1.3]; QGreenland v2.0. B. The pattern of <700 m ice thickness (white) shown around perimeter of the ice sheet, which covers 15.2% of the ice-sheet footprint. C. Where the basal thermal state is likely frozen bedded (white), which covers 37.4% of the ice-sheet footprint (from MacGregor et al., 2022). Basemap topography and bathymetry from Morlighem et al. (2017).

137 Greenland. However, there are drills designed to quickly access the bed in locations where ice  
138 thickness is  $\leq 700$  m (Spector et al., 2017, 2018). The goal of this study is to survey Greenland to  
139 identify sites that are potentially suitable for sub-ice cosmogenic-nuclide measurements using

- Deleted: (
- Deleted: )
- Deleted: (
- Deleted: )
- Deleted: (
- Deleted: )
- Deleted: less than ~
- Formatted: Font color: Text 1
- Formatted: Font color: Text 1

141 two suitable drills in the US Ice Drilling Program’s inventory: the Agile Sub-Ice Geological (ASIG;  
142 Kuhl et al., 2021) drill and the Winke Drill (Boeckmann et al., 2021). Both of these drills can  
143 operate in Greenland. Considering drill specifications, scientific and safety criteria, we identify  
144 multiple suitable sites near the GrIS margin across northern and eastern Greenland. These sites  
145 represent candidate targets for the GreenDrill project supported by the U.S. National Science  
146 Foundation.

147

### 148 **3 Considerations for drilling**

149 The drills currently available from the US Ice Drilling Program that are designed to drill  
150 rock cores beneath tens to hundreds of meters of glacial ice require the bed beneath the ice to  
151 be frozen to its bed. Additional specifications for scientific projects focused on sub-ice samples  
152 obtained via drilling, such as bedrock lithology and site accessibility, further limit suitable areas.  
153 The bedrock lithology of Greenland is varied and is only exposed around the island’s perimeter  
154 and directly observable in only one hand-sample from the base of the GISP2 ice core site. With  
155 only six locations across the GrIS interior where boreholes have reached the bed, there are also  
156 limited direct observations of the ice sheet’s basal thermal state. Below, we compile this and  
157 other necessary information for identifying potential sites for retrieval of rock cores beneath  
158 the GrIS.

159

#### 160 **3.1 Drills**

161 We first briefly outline the technical requirements of the two presently available US Ice  
162 Drilling Program drills designed to drill through ice and into the underlying bedrock: ASIG and  
163 Winkie (Albert et al., 2020). The ASIG Drill is currently designed to drill access holes through ice  
164 <700 m thick and collect bedrock cores several meters long. It requires frozen basal conditions  
165 to ensure that drilling fluid is maintained in the entire borehole across the ice–bed interface.  
166 The ASIG drill was successfully used in West Antarctica near the Pirrit Hills in 2016-2017, where  
167 it drilled through approximately 150 m of ice and collected 8 m of 39-mm-diameter rock core of  
168 excellent quality (Kuhl et al., 2021). Nearly 5 m of ice core was also collected near the ice-  
169 bedrock transition, however, the core quality was poor. The Winkie Drill is capable of drilling

170 120 m of ice and rock (e.g., it can retrieve a 10 m rock core from beneath 110 m of ice); it also  
171 has the requirement of a frozen bed. Given these restrictions, the Winkie Drill is mostly  
172 restricted to frozen-bedded environments very near the GrIS margin, and the ASIG Drill is  
173 suitable to drill in similar environments slightly farther inland.

174

### 175 **3.2 Ice thickness**

176 The large-scale thickness of the GrIS is relatively well known, stemming from several  
177 decades of radar data collection by NASA and European institutions (e.g., Li et al, 2012).  
178 Morlighem et al. (2017) combined airborne radar-sounding-derived ice thickness data with  
179 comprehensive, high-resolution ice motion measurements derived from satellite  
180 interferometric synthetic-aperture radar. This combination of datasets allowed Morlighem et  
181 al. (2017) to employ a mass conservation algorithm (Morlighem et al., 2011; McNabb et al  
182 2012) to calculate ice thickness around the periphery of the GrIS. They produced a map of bed  
183 topography by subtracting ice thickness from a digital elevation model of the ice surface. Mass  
184 conservation works best in areas of fast flow, where uncertainty in flow direction is small and  
185 the glaciers mostly flow due to basal motion (Morlighem et al., 2011). In the interior, where  
186 deformation is likely a more dominant component of ice flow and uncertainty in flow direction  
187 is greater, they employed ordinary kriging to interpolate ice thickness measurements. We use  
188 BedMachine v3 (Morlighem et al., 2017) and ArcGIS to deduce that 15.2% of the GrIS is <700 m  
189 in thickness (Figure 1B).

190

### 191 **3.3 The basal thermal state of the GrIS**

192 Due to the limited number of boreholes that have reached the GrIS bed, its basal  
193 thermal state must presently be estimated from a synthesis of multiple methods. MacGregor et  
194 al. (2016, 2022) combined thermomechanical ice-flow models and inferences from airborne  
195 and satellite remote sensing to constrain where the bed is likely thawed, where it is likely  
196 frozen and where it remains too uncertain to specify, at a spatial resolution of 5 km. The latest  
197 version of this synthesis of the GrIS likely basal thermal state (MacGregor et al., 2022) is shown  
198 in Figure 1C. The map suggests frozen-bedded conditions across 37.4% of the ice sheet, mostly

Deleted: 1

Deleted: 2

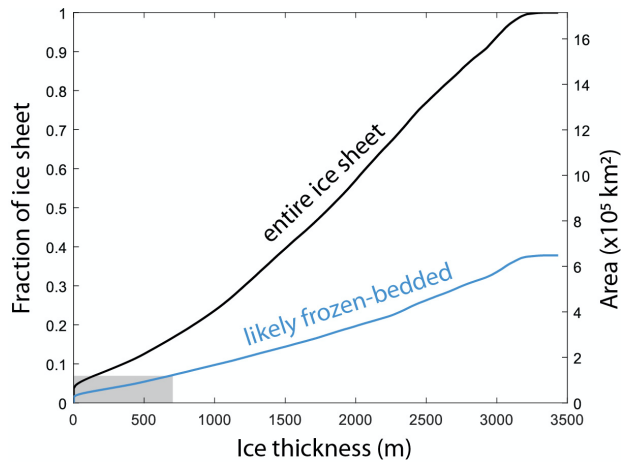


**Figure 2.** Greenland Ice Sheet thickness versus area. Plot shows that only about one-third of the ice sheet by area is likely frozen-bedded, and thus available for subglacial access. The current limit of drills of operating under 700 m ice thickness further reduces available portion of the ice-sheet bed for access (gray area). Note that increasing a drill's depth capability increases the area of the bed available for drilling; the ability to drill into wet-based sections of the ice sheet would significantly increase the area available for drilling.

201 beneath ice divides and parts of North Greenland (Figure 2). The ice margin and near-ice-  
 202 margin areas throughout most of Greenland are largely believed to be thawed, except for a few  
 203 locations across North and East Greenland where frozen-bedded conditions are ubiquitous –  
 204 even near the ice margin. However, there are many areas where the basal thermal state is  
 205 mapped as uncertain (i.e., areas that are inconclusive in terms of their likelihood to be either  
 206 warm-or frozen-bedded), and many of these areas also extend to the ice margin in portions of  
 207 North and East Greenland. Jordan et al. (2018) used radar returns to identify locations of  
 208 probable water at the bed. Although the method could not be applied throughout Greenland  
 209 due to limitations in radar extent and quality, their fine-resolution dataset was included by  
 210 MacGregor et al. (2022). Bedrock weathering textures and landforms observed in landscapes  
 211 occupied by Pleistocene ice sheets reveal sharp transitions between warm- and frozen-bedded  
 212 conditions in the past, particularly in areas of high topographic relief (e.g., Sugden, 1978; Briner  
 213 et al., 2006). Thus, there could be localized patches of frozen-bedded conditions across many

Formatted: Font color: Text 1  
 Formatted: Font color: Text 1



214 areas around the GrIS perimeter that are too small in scale to be suitably represented using the  
 215 methods of Jordan et al. (2018) and MacGregor et al. (2022). Combining likely frozen basal  
 216 conditions with ice thicknesses <700 m results in 6.8% of the bed available for drilling (Figures 2  
 217 and 3A).

218 Finally, prior to drilling, the selected sites should be assessed with geophysical methods  
 219 to further estimate the thermal state of the bed. Existing radar profiles combined with new  
 220 radar and seismic measurements can reduce the uncertainty about the condition of the bed.  
 221 Seismic methods can more confidently measure whether a significant water volume is present  
 222 at the bed, either pooled or within sediment pores (e.g., Kulesa et al., 2017). The reflectivity of  
 223 water or water-laden sediments is significantly different than for frozen sediments. Note that a  
 224 thin layer of water over crystalline bedrock would be difficult to distinguish from frozen ice over  
 225 bedrock.

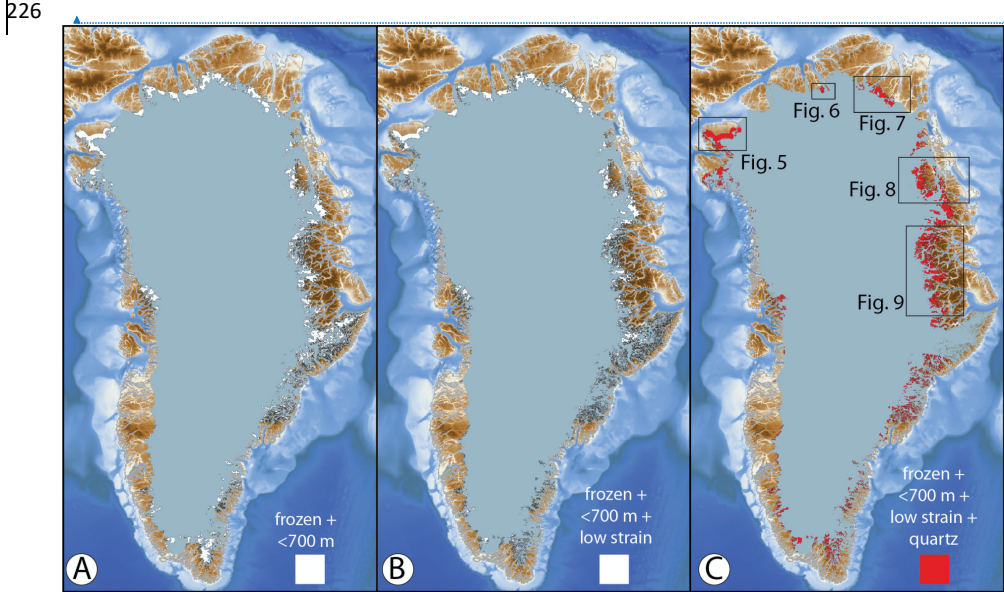


**Figure 3.** A. Portion of the Greenland Ice Sheet bed (6.8%) that are both likely frozen and beneath <700 m of ice. B. Same as in A but which has a low likelihood of surface crevasses (4.8%). C. Same as in B but with likely quartz-bearing lithologies (3.4%). Basemap topography and bathymetry from Morlighem et al. (2017).

227 **3.4 Surface features, safety and site accessibility**

Formatted: Font color: Text 1  
 Formatted: Font color: Text 1

Deleted: (  
 Deleted: )  
 Deleted: (  
 Deleted: )  
 Deleted: (  
 Deleted: )  
 Deleted: 3

229 Because available drills require <700 m ice thickness, the viable areas of interest are  
230 mostly restricted to near the ice margin (Figure 1B). These areas generally have high surface  
231 velocity (>50 m/yr) and spatial variability in surface velocity as ice flow becomes increasingly  
232 influenced by underlying topography (Figure 1A). Consequently, these areas have high strain  
233 rates and can be heavily crevassed, making them some of the most dangerous locations on the  
234 GrIS to work. However, not all ice-marginal areas exhibit high velocity and high strain rates, so  
235 some areas are relatively crevasse free. Surface strain rates derived from GrIS surface velocity  
236 (Figure 1A) can guide site selection for low likelihood of crevassing. In this way, one can address  
237 the criterion of being most likely to be safe for air support and/or access via traverse vehicles.  
238 We use a strain-rate field from Poinar and Andrews (2021) and a threshold value of 0.005/year,  
239 above which crevasses are likely to form (Joughin et al., 2013). This analysis further reduces the  
240 area of the GrIS suitable for drilling from 6.8% to 4.8% (Figure 3B).

### 241 242 **3.5 Cosmogenic nuclides and subglacial geology**

243 An entire family of cosmogenic nuclides are routinely measured in Earth materials. Most  
244 research to date in Earth science, however, has used cosmogenic nuclides produced in quartz:  
245  $^{26}\text{Al}$ ,  $^{14}\text{C}$  and  $^{10}\text{Be}$  (Granger et al., 2013; Briner et al., 2014; Balco, 2020). While there are  
246 cosmogenic nuclides that can be used in mafic lithologies (e.g.,  $^{36}\text{Cl}$ ,  $^3\text{He}$ ) and carbonates (e.g.,  
247  $^{36}\text{Cl}$ ), the advantage of quartz is that the trio of  $^{26}\text{Al}$ ,  $^{14}\text{C}$  and  $^{10}\text{Be}$  can all be measured together  
248 (e.g., Young et al., 2021). These three nuclides have widely spaced half lives, providing a  
249 powerful exposure-burial chronometer well suited for providing direct constraints on ice sheet  
250 history. Additionally,  $^{36}\text{Cl}$  can also be measured in feldspars, and thus targeting felsic-crystalline  
251 lithologies potentially offers a fourth cosmogenic nuclide with a unique half-life for analysis.

252 Because 81% of Greenland's land area lies beneath the ice, bedrock geology has only  
253 been mapped across 19% of Greenland. There is a large degree of uncertainty about the  
254 lithology below the ice sheet. Dawes (2009) inferred the sub-GrIS geology based on information  
255 from six methods: Drill sites, nunataks, coast-to-coast correlation, glacial erratics, detrital  
256 provenance studies and geophysics. For [the purpose of identifying sites for cosmogenic-nuclide  
257 analysis](#), we provide a highly abbreviated overview of this geology with particular attention paid

Deleted: 4

Deleted: A bedrock substrate has advantages over sediment deposits, although cosmogenic nuclide measurements from both are informative. Sediments beneath ice sheets are more easily eroded, deformed, entrained and transported and re-deposited than bedrock. Thus, cosmogenic nuclide concentrations from the sediment grains themselves, which have a transport and deposition history, can be more complicated to interpret than those in bedrock. For targeted sub-GrIS cosmogenic nuclide campaigns, the highest priority sites are those where non-erosive ice rests directly on quartz-bearing bedrock. ¶

Deleted: our

Deleted: s

272 to quartz-bearing lithologies in areas likely to coincide with frozen-bedded conditions. We use  
273 the geologic map of Greenland, available online at <https://www.greenmin.gl/> (Pedersen et al.,  
274 2013; Henriksen et al., 2009). Generally, Greenland mostly consists of Precambrian shield rocks  
275 (both Archean and Proterozoic; largely quartz-bearing) in its southern, western and central  
276 areas. North Greenland consists of Paleozoic basins containing mostly non-quartz-bearing  
277 lithologies. East and Northeast Greenland comprise the Caladonian fold belt and a complex  
278 pattern of Proterozoic rocks of mixed lithology, although these are thought to be mainly limited  
279 to the island's periphery. Portions of the central east and central west coasts of Greenland  
280 contain Paleogene volcanic lithologies that may connect beneath the central GrIS. North  
281 Greenland generally encompasses the highest proportion of the margin and near-margin areas  
282 thought to be frozen-bedded; however, carbonate and other non-quartz-bearing lithologies  
283 dominate these areas. We use the geologic map of Greenland to categorize bedrock lithology  
284 into quartz-bearing and non-quartz-bearing units (Figure 4). We remove the ice-marginal areas  
285 adjacent to carbonate and volcanic lithologies from consideration, which reduces the target  
286 area from 4.8% to 3.4% of the GrIS (Figure 3C).

287 Cosmogenic nuclide analyses made in a depth profile below the ice-bed interface yields  
288 important information. Measurements in a rock core spanning a meter or more, for example,  
289 can allow one to easily identify whether or not the current ice-bed interface has been eroded  
290 and/or covered by snow, ice or sediment for long durations (e.g. Schaefer et al., 2016). On the  
291 other hand, one cannot determine with surface-only samples whether a surface has been  
292 impacted by minor erosion and/or burial by snow, ice or sediment. Thus, analysis of bedrock  
293 cores is most important for elucidating ice sheet histories from cosmogenic-nuclide inventories.  
294 Furthermore, cores spanning several meters and including depths dominated by muon  
295 production have the added advantage of constraining orbital-scale term exhumation histories  
296 (e.g., Balter-Kennedy et al., 2021).

297 Sampling from a bedrock substrate has advantages over samples from sediment  
298 deposits, although cosmogenic nuclide measurements from both are informative. Sediments  
299 beneath ice sheets are more easily eroded, deformed, entrained, transported and re-deposited  
300 than bedrock. Thus, cosmogenic nuclide concentrations from the sediment grains themselves,

Deleted: e

302 [which have a transport and deposition history, are more complicated to interpret than those in](#)  
303 [bedrock. Furthermore, cold-based ice that flows atop sediment sections can more easily erode](#)  
304 [a sediment surface \(via entrainment processes\) than in bedrock substrates. Thus, not only is a](#)  
305 [cosmogenic signal in sediments derived from each individual grain's exposure and burial](#)  
306 [elsewhere \(that are later amalgamated into a single deposit\), but the ice-bed itself may not](#)  
307 [represent a prior land "surface." Thus, sediment samples could be from an arbitrary depth](#)  
308 [below a paleo-surface. The depositional environment of sediment is also important. If ice](#)  
309 [overlies a fluvial sediment sequence, then the cosmogenic nuclide inventory is highly likely to](#)  
310 [have a complicated genesis, and thus a more complicated interpretation. On the other hand, if](#)  
311 [the sediment is saprolite or regolith, and largely formed in-situ, then its cosmogenic nuclide](#)  
312 [inventory likely would be more straight forward to interpret. In any case, for targeted sub-GrIS](#)  
313 [cosmogenic nuclide campaigns, the highest priority sites are those where non-erosive ice rests](#)  
314 [directly on quartz-bearing bedrock.](#)

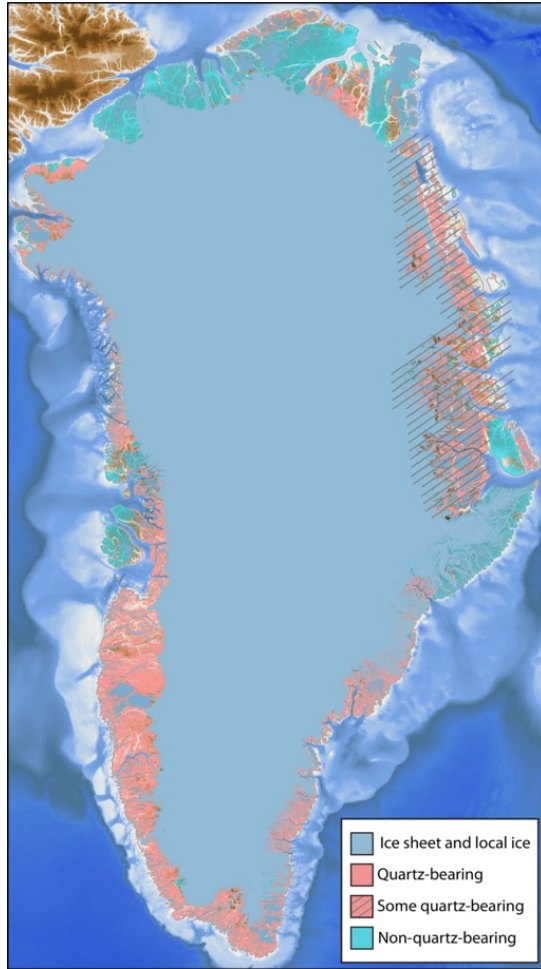
315 [How to maximize the chance of drilling into bedrock?](#) Site selection is aided by airborne  
316 radar sounding data obtained by NASA Operation IceBridge. Existing surveys of the ice sheet  
317 bed are inadequate for identifying every low topographic swale that could potentially be  
318 sediment filled, particularly between radar flight lines. However, by avoiding valleys and low  
319 areas and instead opting for mountain summits or plateaus, we can increase the likelihood of  
320 drilling into bedrock with thin or no sediment cover. Although not always the case, in most  
321 areas of Greenland that are ice free today, bare bedrock surfaces generally exist in higher  
322 proportion on hilltops and uplands, as opposed to low-lying areas and valley bottoms. Thus,  
323 choosing sites along radar flight lines ensures the most reliable knowledge of bed topography  
324 and ice thickness at a candidate drill site.

**Deleted:** In addition to lithology considerations, one may prefer to generate depth profiles of cosmogenic nuclides in bedrock as opposed to in sediment, as mentioned above.

**Deleted:**

**Deleted:** n

331



Formatted: Font color: Text 1

Formatted: Font color: Text 1

**Figure 4.** Simplified bedrock geology map of Greenland, showing lithology sub-divided into probably quartz-bearing rocks, some quartz bearing lithologies and probably non-quartz-bearing rocks. From <https://www.greenmin.gl/>. Basemap topography and bathymetry from Morlighem et al. (2017).

332 **3.6 Strategizing drill site selection related to scientific motivation**

Deleted: 5

333 Having applied above the drilling and geologic requirements for site selection, we next  
334 consider the scientific progress that could be realized from the analysis of bed materials at a

336 particular site. With the goal of constraining Pleistocene GrlS history in mind, we consider four  
337 primary criteria.

338 First, the best sites should be robust monitors of past ice-sheet margin change. There  
339 could be regions, such as high-elevation terrain (e.g., in mountainous East Greenland) that meet  
340 the technical criteria but retain local ice cover during times of reduced ice-sheet configurations,  
341 complicating the link between the study site and broader GrlS change. There could also be sites  
342 that are part of the GrlS but are better conceived of as separate ice domes connected to the ice  
343 sheet via a saddle; these 'local' domes may persist longer than the adjacent ice sheet during  
344 interglacial periods as disconnected ice caps (e.g., Prudhoe Dome, Figure 5). [Ice-sheet modeling  
345 should be used to help guide site selection \(Keisling et al., 2022\).](#)

346 Second, to best capitalize on new measurements of cosmogenic nuclide signatures of  
347 past ice sheet changes (Spector et al., 2018; Keisling et al., 2022), sites should be sought that  
348 have persistent frozen-bedded conditions throughout glacial–interglacial cycles. These sites  
349 should favor preservation of cosmogenic nuclides at the ice–bed surface and reduce the  
350 likelihood of significant periods of time with subglacial erosion that removes the cosmogenic  
351 nuclide inventory. [At sites where sub-glacial conditions favor erosion, cosmogenic nuclides  
352 would be largely absent, hence removing one of the main reasons for obtaining sub-ice bedrock  
353 samples.](#) Identifying these sites could be based on a combination of selecting presently frozen  
354 bedded areas, favoring high-elevation locations or ice divide areas likely to be frozen bedded  
355 during past larger ice-sheet configurations, and evaluating paleo ice-sheet models to find ideal  
356 drilling locations.

357 Third, there may be some sites that are more sensitive monitors of reduced ice extent  
358 than others. For example, while some sites at 600 m ice thickness today may become ice free at  
359 under 5% reduction in ice-sheet mass, others may not become ice-free until a substantially  
360 greater reduction in mass. Using numerical ice-sheet models could greatly assist site selection  
361 and help to further explore sites that meet the technical requirements for their potential to  
362 constrain past ice sheet configurations (Keisling et al., 2022).

363 Fourth, some ice-sheet margin areas that include large, fast-flowing outlet glaciers with  
364 beds below sea level (e.g., near Jakobshavn Isbræ, Petermann Glacier, Northeast Greenland Ice

365 Stream), could potentially 'collapse' at rates faster than other ice sheet margin areas. Thus,  
366 sites neighboring these regions, such as the Northeast Greenland Ice Stream, could not only  
367 serve as a binary signal of ice sheet presence/absence, but could help to elucidate the response  
368 of major outlet glaciers influenced by ice-ocean interactions to past climate forcing. Does the  
369 Northeast Greenland Ice Stream collapse during past warm times and exhibit proportionally  
370 more ice sheet recession than other ice-sheet sectors? Sites adjacent to the Northeast  
371 Greenland Ice Stream could help resolve this question.

372 [Finally, additional considerations relating to field season planning could lead to meeting](#)  
373 [scientific goals most efficiently. Multiple drill cores along transects \(even including sites beyond](#)  
374 [the present – ephemeral – position of the ice-sheet margin\) could boost confidence in](#)  
375 [constraining past ice-sheet dimensions through time. For example, a site that is presently](#)  
376 [covered by 100 m of ice, may have been ice-free during the Holocene, whereas a 400-m-thick](#)  
377 [site farther inland was not; thus, one could better constrain the position of the ice margin](#)  
378 [during the middle Holocene. Additionally, using the ASIG Drill, there may be enough time in a](#)  
379 [field season to acquire one or two drill cores from thicker ice sites \(e.g., 500-700 m\), versus](#)  
380 [obtaining many drill cores in a single season from ~100m-thick sites using the Winke Drill. The](#)  
381 [optimal sampling strategy depends on several factors that relate to a particular scientific](#)  
382 [objective.](#)

#### 383 384 4. Areas suitable for drilling using ASIG

385 We synthesized the information discussed above to derive a map of candidate areas  
386 across the GrIS for drilling (Figure 3C). While only 3.4% of the GrIS bed is well suited for  
387 subglacial access for [the purpose of cosmogenic-nuclide analysis](#), there are several promising  
388 candidate sites: (1) Northwest Greenland, specifically the metamorphic lithologies of the  
389 Ellesmere-Inglefield Province in Prudhoe Land-Inglefield Land; (2) Two regions in North  
390 Greenland: a small area around the head of Victoria Fjord that likely exposes metamorphic  
391 lithologies of the Victoria Province and an area adjacent to Mylius-Erichsen Land in eastern  
392 North Greenland that contains siliciclastic sedimentary units; (3) Dronning Louise Land in  
393 Northeast Greenland, where both crystalline and siliciclastic lithologies are present; and 4)

Deleted: -thickness site

Deleted:

Deleted: ice-

Deleted: ness

Deleted:

Deleted: ice

Deleted: -

Deleted: ness

Deleted: a number of

Deleted: ¶

Deleted: our

Deleted: s

406 central East Greenland, where the GrlS flows through alpine terrain of mixed lithology en route  
407 to the headwaters of the Scoresby Sund, Kong Oscar Fjord and Kejser Franz Joseph Fjord  
408 systems. There are additional small areas scattered around the periphery of the GrlS; however,  
409 most areas are in alpine-style, icefield-type settings, or lie in small areas between outlet  
410 glaciers. [In these additional small areas, however, existing uncertainties in available datasets](#)  
411 [\(e.g., ice sheet thickness, basal temperature, etc.\) means that drilling there is potentially riskier](#)  
412 [than in larger patches of the bed that meet drilling requirements.](#)

413

#### 414 **4.1 Northwest Greenland: Prudhoe Land and Inglefield Land**

415 In Northwest Greenland, the ice sheet in Prudhoe Land and Inglefield Land has broad  
416 areas that meet the technical, safety and lithology criteria (Figures 3C and 5). Here, there are  
417 basement rocks consisting of Proterozoic metamorphic lithologies. Proportionally much of the  
418 region contains quartz-bearing metamorphic rocks (e.g., paragneiss), albeit with varying quartz  
419 content, and in some cases with bands of marble and other potentially non-quartz-bearing  
420 units (e.g., syenite, amphibolite; Henriksen et al., 2009). Further, the ice sheet has been  
421 surveyed extensively by NASA's Operation IceBridge and abundant radar data exist. The ice  
422 sheet margin adjacent to Inglefield Land, spanning between Hiawatha Crater and Prudhoe  
423 Dome, is roughly parabolic in profile and rather uniform in velocity, with surface speeds mostly  
424 ranging from 3–10 m yr<sup>-1</sup>. The topography of the ice sheet bed is low-relief, potentially making  
425 it difficult to identify small hills and swales where the substrate is less or more likely to host  
426 sediment. The landscape fronting the ice is largely bedrock, or bedrock overlain by surface  
427 blocks either frost-riven or slightly modified by former glaciation. In a few areas, alluvium or  
428 glacial deposits exist at the surface. Prudhoe Dome itself (Figure 5) has a thickness of ~500 m at  
429 a summit ridge that rests along a topographic high above a bed elevation of ~800 m asl. The  
430 velocities in the summit region of Prudhoe Dome range up to ~20 m yr<sup>-1</sup>. The Prudhoe Dome  
431 summit is a promising place to drill, with a high probability of encountering bedrock at the ice  
432 sheet bed. However, upon deglaciation, the site may maintain local ice isolated from the inland



433 ice, potentially fueled by snowfall due to its proximity to Baffin Bay. [Ice sheet modeling could](#)  
434 [be used to detect inland \(ice sheet\) versus peripheral \(local\) ice survival in locations like this.](#)

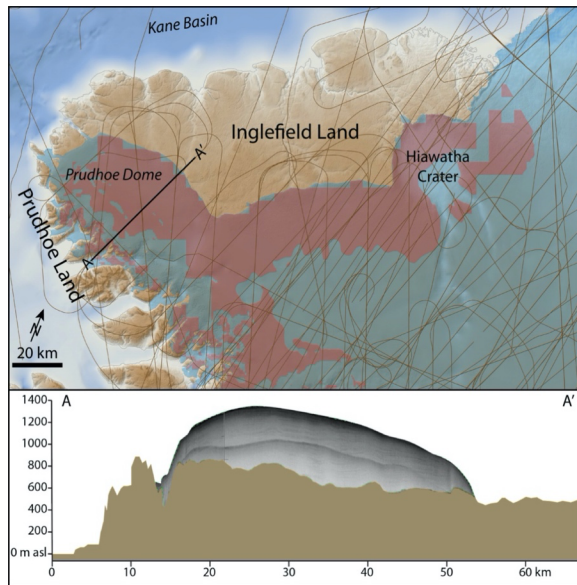


**Figure 5.** Top panel shows areas that meet drilling requirements (shown in red) in NW Greenland. The Greenland Ice Sheet is depicted in light blue, and NASA Operation IceBridge (OIB) flight lines are shown as thin brown lines. Bottom panel shows OIB radar of Prudhoe Dome along A-A', with topography, the ice-sheet bed and the ice-sheet surface from radar collected in 2017; the mid-ice-sheet reflector is the surface multiple. Basemap topography and bathymetry from Morlighem et al. (2017).

Formatted: Font color: Text 1  
Formatted: Font color: Text 1

Deleted:

435  
436 **4.2 North Greenland: Victoria Fjord**

437 Most of North Greenland is dominated by sedimentary rocks of the lower Paleozoic  
438 Franklinian Basin not well suited for providing the hard, quartz-bearing lithologies that work  
439 best for in-situ cosmogenic nuclide analysis (Henriksen et al., 2009). At the head of Victoria  
440 Fjord (Figure 6A), however, Henriksen and Jepsen (1985) describe isolated outcrops of  
441 crystalline basement in otherwise non-quartz-bearing sedimentary-rock-dominated North  
442 Greenland. The crystalline rocks, mostly orthogneiss, comprise several nunataks in Victoria  
443 Fjord, and additionally crop out in the bottom of two valleys between C.H. Ostenfeld and Ryder  
444 glaciers (Figure 6B). The sedimentary formations consist of Neoproterozoic through Silurian  
445 lithologies composed of near-horizontally bedded shale, siltstone and abundant carbonate

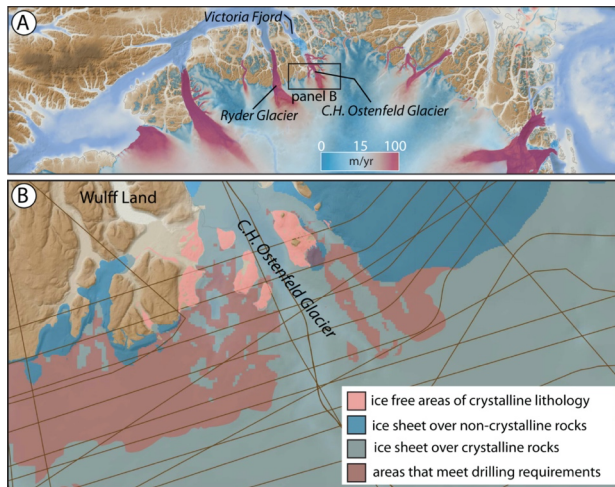


**Figure 6.** A. North Greenland showing ice sheet surface velocity; velocity from Greenland Ice Sheet velocity map from Sentinel-1, winter campaign 2019/2020 [version 1.3]; QGreenland v2.0. B. Areas that meet drilling requirements with a focus on bedrock lithology: bright blue are areas under the ice sheet with non-quartz bearing lithologies whereas the more muted blue colors depict our estimate of where there are quartz-bearing lithologies at the ice bed. Pink areas are quartz-bearing lithologies beyond the ice margin, and shown in muted red color are the areas that meet the drilling requirements. NASA Operation IceBridge (OIB) flight lines are shown as thin brown lines. Basemap topography and bathymetry from Morlighem et al. (2017).

Deleted:

446 units. The outcrop pattern is one of crystalline rocks exposed at lower elevations where the  
 447 GrIS had eroded away the overlying sub-horizontal sedimentary rocks, or cap rocks. Overall, the  
 448 outcrop of these quartz-bearing lithologies is promising for their existence at the ice-sheet bed  
 449 south of the ice sheet margin. However, because there are topographic highs along the GrIS  
 450 bed south of the margin, blindly drilling into areas that meet the other technical requirements  
 451 could lead to encountering cap rocks. For this region, we perform an additional step to estimate  
 452 where the bed south of the ice margin may be crystalline vs. sedimentary. To project the  
 453 crystalline/cap rock contact southward under the ice sheet, we use the contact between  
 454 crystalline rocks and the overlying cap rocks in exposed areas to perform a “3-point problem”  
 455 an established method for determining the strike and dip of a plane based on geologic outcrop  
 456 patterns. As observed by Henriksen and Jepsen (1985), the contact dips gently to the north, and  
 457 the plane that we calculated in ArcGIS confirms this. Our estimation reveals crystalline rocks

Formatted: Font color: Text 1

Formatted: Font color: Text 1

Deleted: created

459 outcropping in topographic low areas, and cap rocks outcropping in topographic high areas  
 460 (Figure 6B). Our estimated contact is simplistic, as there may be folding and faulting that limit  
 461 the accuracy of this extrapolation. However, this solution provides a straightforward estimate  
 462 for where crystalline rocks may exist at the ice–bed interface near the head of Victoria Fjord.  
 463 Using this information, along with Operation IceBridge flight lines and in combination with  
 464 areas that meet the other technical and safety requirements, indicates promising areas to drill  
 465 to the southwest of the onset zone of C.H. Ostenfeld Gletscher (Figure 6B).

466

467 **4.3 North Greenland: Mylius-Erichsen Land**

468 In eastern North Greenland there is an ~100-km stretch of ice margin in Mylius-Erichsen  
 469 Land (Figure 7) that lies over quartz-bearing sedimentary lithologies of the Proterozoic  
 470 Independence Fjord Group (Henriksen et al., 2009). The rocks in this region contain near-  
 471 horizontally bedded siltstones, sandstones, and quartzites intruded by Mesoproterozoic

Formatted: Font color: Text 1  
 Formatted: Font color: Text 1

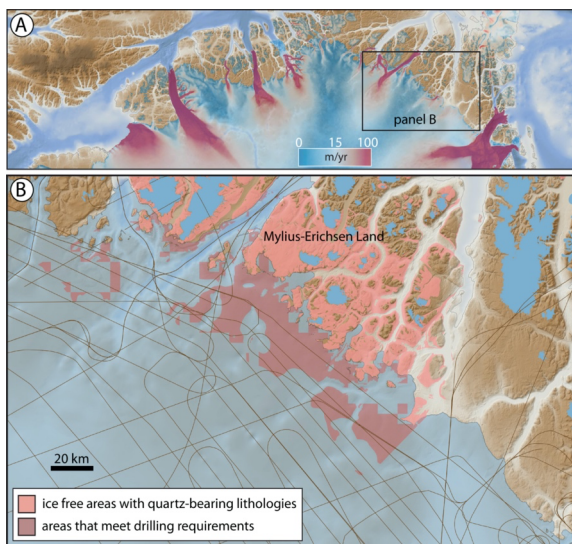


**Figure 7.** A. North Greenland showing ice sheet surface velocity; velocity from Greenland Ice Sheet velocity map from Sentinel-1, winter campaign 2019/2020 [version 1.3]; QGreenland v2.0. B. Mylius-Erichsen Land showing areas that meet drilling requirements, with pink areas representing quartz-bearing sedimentary formations (with mafic intrusives) beyond the ice margin. NASA Operation IceBridge (OIB) flight lines are shown as thin brown lines. Basemap topography and bathymetry from Morlighem et al. (2017).

Deleted:

472 dolerite sills, dikes and stocks. Significant portions of the ice sheet in this region meet the  
473 technical and safety requirements for drilling, so the suitability for developing GrlS histories  
474 rests mostly on the likelihood of encountering preferred lithologies. The pattern on the geologic  
475 map and the unit description of the rock formations in the area indicate that the abundance of  
476 mafic intrusions mean that drilling has a reasonable chance of encountering non-quartz-bearing  
477 lithologies. The region has relatively sparse radar [lines](#) that cross drilling-suitable areas  
478 compared to other parts of Greenland, narrowing the choices of drill sites that have tight  
479 constraints on ice thickness and bed shape.

Deleted: data

480

#### 481 **4.4 Northeast Greenland: Dronning Louise Land**

482 The nunatak region of Dronning Louise Land, Northeast Greenland, contains broad areas  
483 that meet the technical requirements for subglacial drilling (Figure 8). The bedrock geology is  
484 part of the Caledonian fold belt and contains abundant structures that formed during the  
485 Caledonian Orogeny (Ordovician-Devonian) leading to the juxtaposition of crystalline and  
486 younger sedimentary rock formations in a complicated map pattern (Henriksen et al., 2009;  
487 Strachan et al., 2018). The broadest regions that meet [the](#) technical criteria and are most  
488 favorable for drilling lie on the western (inland) portion of the coastal mountain ranges. Here,  
489 nunataks exist 25-30 km west of the coastal mountains and provide information on the bedrock  
490 geology most relevant to potential drilling areas. The lithologies are similar to and have been  
491 correlated with the Independence Fjord Group found in Mylius-Erichsen Land. Specifically, the  
492 local unit that comprises inland nunataks (the Trekant Series) consists largely of quartzitic and  
493 feldspathic sandstone and conglomerate with intercalated siltstone and mudstone. Bedrock  
494 mapping in the nearby coastal mountains also reveals Mesoproterozoic dolerite intrusions.  
495 Sparse radar data limits potential drill sites with close constraints on ice thickness and bed  
496 shape. Yet, the region does have potential for tapping into quartz-bearing units and due to its  
497 proximity to the Northeast Greenland Ice Stream, sub-ice cosmogenic nuclide analyses from the  
498 area could yield important constraints on Northeast Greenland Ice Stream history. Finally, the  
499 possibility that high-elevation areas remain glaciated by local ice after inland ice recedes should  
500 not be ignored. Many of the sub-ice drilling targets are >1000 m asl, near twentieth century

Deleted: our

503 snowline elevations. [To reduce the chances of drilling a site that is occupied by local ice once](#)  
504 [inland ice recedes, one could assess snowline elevation gradients using the presence/absence](#)  
505 [of ice caps in peripheral mountains along this coastline. Preliminary analysis shows that](#)  
506 [snowline elevations increase inland. Extrapolating these gradients to sub-ice areas suitable for](#)  
507 [drilling could help to guide drill site selection by identifying sites with elevations lower than](#)  
508 [projected snowline altitudes.](#) [In this way](#), targeting lower-elevation parts of the sub-ice terrain  
509 could be advantageous given [the goal of monitoring](#) GrIS history. [Additional radar surveys over](#)  
510 key areas would be useful for tightening constraints on ice thickness and bed topography over  
511 the frozen-bedded patches of Dronning Louise Land.

512

#### 513 4.5 East Greenland

Deleted: Thus

Deleted: our

Deleted: to

Deleted: The region has relatively sparse radar data coverage, suggesting that a...

519 A final place to highlight is central East Greenland, where – similar to Dronning Louise  
 520 Land – the GrIS abuts and flows through alpine terrain. The western (inland) flank of these  
 521 mountains has dozens of isolated areas that meet the technical requirements of drilling to the  
 522 bed (Figure 9). Like the other areas throughout East and Northeast Greenland, the bedrock  
 523 geology is highly variable. The headwaters of the Scoresby Sund, Kong Oscar Fjord and Kejser

Formatted: Font color: Text 1

Formatted: Font color: Text 1

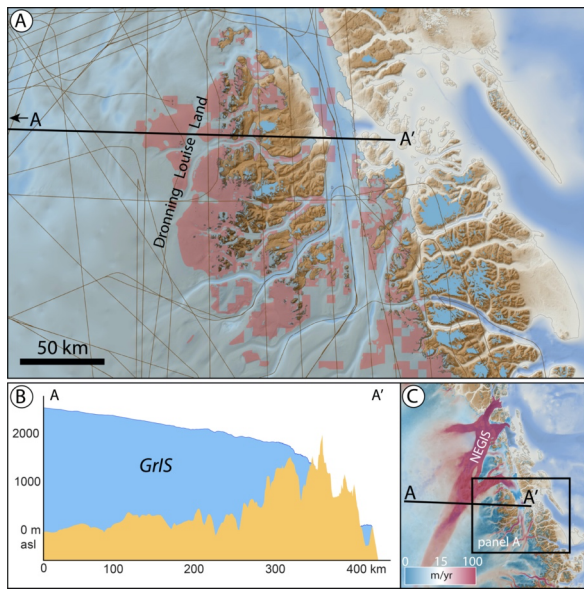


**Figure 8.** A. Dronning Louise Land showing areas that meet drill requirements; NASA Operation IceBridge (OIB) flight lines are shown as thin brown lines. B. Topographic profile of bed and GrIS surface from Bed Machine v3 (Morlighem et al., 2017); cross section line shown in panel C. C. NE Greenland with surface velocity showing NEGIS and location of panel A; velocity from Greenland Ice Sheet velocity map from Sentinel-1, winter campaign 2019/2020 [version 1.3]; QGreenland v2.0. Basemap topography and bathymetry from Morlighem et al. (2017).

Deleted:

524 Franz Joseph Fjord systems have a complicated geology relating to the Caledonian Orogen,  
 525 consisting of Paleoproterozoic crystalline metamorphic and sedimentary formations that are in  
 526 turn slightly metamorphosed (Henriksson et al., 2009). In terms of finding quartz-bearing rocks  
 527 most suitable for cosmogenic nuclide analysis, the region is heterogeneously made up of  
 528 quartz-bearing (e.g., orthogneiss) and non-quartz-bearing formations (various fine-grained  
 529 siliciclastic lithologies with occasional mafic intrusions). Inland nunataks provide knowledge of  
 530 bedrock geology most proximal to potential drill locations and are largely composed of pelitic

531 lithologies (e.g., metamorphosed mudstones). Looking closely at nunatak lithologies reveals  
 532 some westernmost nunataks of orthogneiss composition, such as inland of J.L. Mowinckel Land  
 533 (Figure 9), making the areas in this region that meet the technical requirement promising. A  
 534 consideration with the potential drilling locations in central East Greenland, again, is the  
 535 likelihood that they are deglaciated with the recession of inland ice, as opposed to retaining  
 536 local ice cover. Airborne radar data are also sparse there, so care would be needed to select  
 537 sites with the best constraints of ice thickness and bed shape.

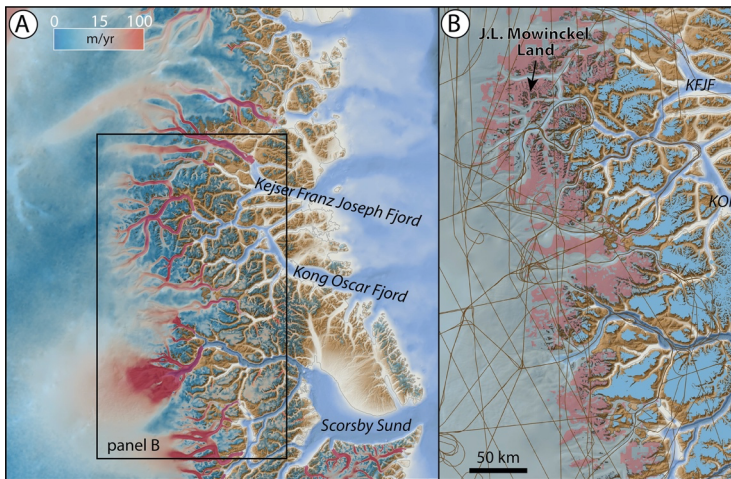


**Figure 9.** A. East Greenland showing GrIS flowing through alpine terrain; surface velocity highlights major outlets; velocity from Greenland Ice Sheet velocity map from Sentinel-1, winter campaign 2019/2020 [version 1.3]; QGreenland v2.0. B. Portion of East Greenland that includes the most areas that meet the technical requirements of drilling to the bed. Basemap topography and bathymetry from Morlighem et al. (2017).

538  
 539 **5. Conclusions**

540 The purpose of this study is to identify potential targets for subglacial drilling with  
 541 cosmogenic nuclide analysis in mind. We find that only 3.4% of the GrIS is well suited for  
 542 cosmogenic-nuclide analysis of bed materials using existing drills available from the US Ice  
 543 Drilling Program and highlight five promising locations in northern and eastern Greenland.  
 544 Future advances in drill capability, such as the ability to drill through thicker or wet-based ice,  
 545 would significantly increase the area available for drilling (Figure 2).

Formatted: Font color: Text 1  
 Formatted: Font color: Text 1

Deleted: <object>  
 Formatted: Font color: Text 1  
 Formatted: Font color: Text 1  
 Deleted: Each of the two cases in Greenland in which cosmogenic nuclides have been analyzed in sub-ice material has led to significant insights into the history of the GrIS (Schaefer et al., 2016; Christ et al., 2020). Some of this new information – the time periods and duration of the Quaternary Period in which the GrIS was significantly reduced and/or largely absent – led to a reevaluation of the existing paradigm of GrIS expansion at the Quaternary boundary and general stability thereafter (Briner et al., 2017). This paradigm-shifting information from the GISP2 and Camp Century sites was based on archived material that was not collected specifically for sub-ice cosmogenic nuclide analysis.  
 Formatted: Font: Not Italic, Font color: Text 1  
 Formatted: Font color: Text 1  
 Deleted: future

561 In addition to obtaining drill cores of rock or sediment from the ice sheet bed, samples  
562 of other basal material would also benefit the research community. Basal ice is valuable for (1)  
563 measuring trace gasses to obtain basal ice age (Bender et al., 2010, Yau et al., 2016b), (2)  
564 detrital cosmogenic nuclide analysis of its mineral component (Bierman et al., 2014), and (3)  
565 ancient DNA and biomarkers in organic compounds (Willerslev et al., 2007). Boreholes  
566 themselves that are the product of drilling can be instrumented, resulting in direct  
567 measurements of basal heat flux values that would provide additional constraints on the basal  
568 thermal state of the GrIS (e.g., MacGregor et al., 2022; Colgan et al., 2021) and the history of  
569 the Iceland hotspot (e.g., Rogozhina et al., 2016). Finally, precise sampling at the ice-bed  
570 interface could lead to the discovery of ancient soils that plausibly exist in areas targeted for  
571 drilling that are frozen-bedded for long periods. Such samples may be useful for a variety of  
572 studies including ancient DNA, macrofossil, and biomarker analyses. Additionally, with proper  
573 precautions, the uppermost few millimeters of the bed can be preserved in light-free conditions  
574 and used to measure for luminescence dating, providing an additional chronometer of past ice-  
575 sheet presence/absence (e.g., Christ et al., 2021).

576 [Pairing sub-ice cosmogenic-nuclide analysis with ice-sheet modeling is an important step](#)  
577 [\(Spector et al., 2018\). Ice-sheet model simulations have the ability to scale information from](#)  
578 [single drill sites, or transects of sites, to the entire GrIS. Likewise, results from ice-sheet](#)  
579 [modeling can help identify which potential drill sites are most sensitive to overall ice sheet](#)  
580 [mass balance, thus help to prioritize sites or to assemble a strategically chosen group of sites.](#)  
581 [Finally, high resolution ice-sheet models with fine meshes in areas of peripheral mountainous](#)  
582 [topography could help with 'local ice survival' issues that could complicate cosmogenic-nuclide](#)  
583 [records from areas where alpine topography is smothered by the GrIS.](#)

584 [In our companion paper \(Keisling et al., 2022\), we use an ensemble of ice-sheet](#)  
585 [simulations to illustrate deglaciation styles around the GrIS. The results reveal how much sea](#)  
586 [level equivalent the GrIS has lost as each perimeter site becomes ice free, many of which are](#)  
587 [reachable by the ASIG drill. The geometry of ice-sheet retreat depends on a number of ice-](#)  
588 [sheet model parameters, including climate forcing, lapse rate, model initialization, lithosphere](#)  
589 [response, etc. We found that some locations become ice free after a similar amount of ice loss](#)



590 [regardless of the uncertainty in these parameters, whereas other locations experience a range](#)  
591 [of ice-cover histories depending on the model parameters. Our results demonstrate how](#)  
592 [numerical models can provide another tool to guide site selection by identifying locations](#)  
593 [where bedrock-derived evidence for ice-free conditions tells us something concrete about ice-](#)  
594 [sheet size and volume. More observational data of past GrIS change, such as cosmogenic](#)  
595 [nuclide analyses, will improve the model-based estimates by identifying the deglaciation styles](#)  
596 [that are the most realistic, thereby constraining parametric uncertainty. In turn, as models](#)  
597 [become more competent, they have the ability to scale single drill-site \(or transects of sub-ice](#)  
598 [drill sites\) information into a broader picture of regional, or whole, GrIS change. As both of](#)  
599 [these tools improve, taking an integrated approach offers the greatest potential for leveraging](#)  
600 [new breakthroughs into societally relevant information about ice-sheet history and stability.](#)

601 In summary, we consider this study, and ideally drilling efforts taking place in one or  
602 more of these candidate sites, as only one of several next steps in the exploration of the GrIS  
603 bed [and in providing useful data for improving ice-sheet models](#). We recommend development  
604 of drills that can penetrate thicker ice and potentially ice where the bed is thawed. This could  
605 be done by modifying existing drill technology (e.g., Timoney et al., 2020; Goodge et al., 2021)  
606 or require the development of entirely new drills. Expanding the area of the GrIS available for  
607 subglacial drilling would broaden the range of scientific questions that could be addressed  
608 regarding GrIS history and the range of possible targets. The application of cosmogenic nuclide  
609 analysis of subglacial materials could then move beyond constraining GrIS history during  
610 periods when it is only slightly smaller (~90%) than its present configuration to constraining  
611 times of significant reduction (~<10%). Additionally, there would be more resolving power for a  
612 fuller range of scientific questions, such as what shape the GrIS takes during past interglacials  
613 (Plach et al., 2018; Domingo et al., 2020), where ice dynamics may influence large-scale retreat  
614 (Aschwanden et al., 2019), or where there are packages of subglacial lake sediments (e.g.,  
615 Keisling et al., 2020; Paxman et al., 2021) or unique geologic structures (Kjær et al., 2018;  
616 MacGregor et al., 2019). Evolving drilling techniques and analyses like this pave the way for  
617 targeted exploration of subglacial bed environments, a new frontier in ice sheet and sea level  
618 science.

619

620 **Author contribution**

621 JB led the analysis and writing. CW led geographic-information-system computations. All  
622 authors contributed to discussions that resulted in the ideas and analysis presented in this  
623 manuscript, and all authors contributed to writing and presentation. [We thank Greg Balco and](#)  
624 [an anonymous referee for important suggestions that helped to improve this paper.](#)

625

626 **Acknowledgement**

627 This work was funded with NSF grant 1933938 (JPB) and 1933927 (NEY, JMS, BAK).

628

629 **References**

630

631 Albert, M. R., Slawny, K. R., Boeckmann, G. V., Gibson, C. J., Johnson, J. A., Makinson, K., and Rix, J.: Recent  
632 innovations in drilling in ice, 2020.

633

634 Aschwanden, A., Fahnestock Mark, A., Truffer, M., Brinkerhoff Douglas, J., Hock, R., Khroulev, C., Mottram, R.,  
635 and Khan, S. A.: Contribution of the Greenland Ice Sheet to sea level over the next millennium, *Science*  
636 *Advances*, 5, eaav9396, 10.1126/sciadv.aav9396, 2019.

637

638 Balco, G.: Glacier Change and Paleoclimate Applications of Cosmogenic-Nuclide Exposure Dating, *Annual*  
639 *Review of Earth and Planetary Sciences*, 48, 21-48, 10.1146/annurev-earth-081619-052609, 2020.

640

641 Balter-Kennedy, A., Young, N. E., Briner, J. P., Graham, B. L., and Schaefer, J. M.: Centennial- and Orbital-Scale  
642 Erosion Beneath the Greenland Ice Sheet Near Jakobshavn Isbræ, *Journal of Geophysical Research: Earth*  
643 *Surface*, 126, e2021JF006429, <https://doi.org/10.1029/2021JF006429>, 2021.

644

645 Bender, M. L., Burgess, E., Alley, R. B., Barnett, B., and Clow, G. D.: On the nature of the dirty ice at the  
646 bottom of the GISP2 ice core, *Earth and Planetary Science Letters*, 299, 466-473,  
647 <https://doi.org/10.1016/j.epsl.2010.09.033>, 2010.

648

649 Bierman Paul, R., Corbett Lee, B., Graly Joseph, A., Neumann Thomas, A., Lini, A., Crosby Benjamin, T., and  
650 Rood Dylan, H.: Preservation of a Preglacial Landscape Under the Center of the Greenland Ice Sheet, *Science*,  
651 344, 402-405, 10.1126/science.1249047, 2014.

652

653 Bierman, P. R., Shakun, J. D., Corbett, L. B., Zimmerman, S. R., and Rood, D. H.: A persistent and dynamic East  
654 Greenland Ice Sheet over the past 7.5 million years, *Nature*, 540, 256-260, 10.1038/nature20147, 2016.

655

656 Briner, J. P., Cuzzone, J. K., Badgeley, J. A., Young, N. E., Steig, E. J., Morlighem, M., Schlegel, N.-J., Hakim, G.  
657 J., Schaefer, J. M., Johnson, J. V., Lesnek, A. J., Thomas, E. K., Allan, E., Bennike, O., Cluett, A. A., Csatho, B., de  
658 Vernal, A., Downs, J., Larour, E., and Nowicki, S.: Rate of mass loss from the Greenland Ice Sheet will exceed  
659 Holocene values this century, *Nature*, 586, 70-74, 10.1038/s41586-020-2742-6, 2020.

660

661 Briner, J. P., Lifton, N. A., Miller, G. H., Refsnider, K., Anderson, R., and Finkel, R.: Using in situ cosmogenic  
662 <sup>10</sup>Be, <sup>14</sup>C, and <sup>26</sup>Al to decipher the history of polythermal ice sheets on Baffin Island, Arctic Canada,  
663 *Quaternary Geochronology*, 19, 4-13, <https://doi.org/10.1016/j.quageo.2012.11.005>, 2014.

664

665 Briner, J. P., Miller, G. H., Davis, P. T., and Finkel, R. C.: Cosmogenic radionuclides from fiord landscapes  
666 support differential erosion by overriding ice sheets, *GSA Bulletin*, 118, 406-420, 10.1130/B25716.1, 2006.

667

668 Briner, J. P., Stewart, H. A. M., Young, N. E., Philipps, W., and Losee, S.: Using proglacial-threshold lakes to  
669 constrain fluctuations of the Jakobshavn Isbræ ice margin, western Greenland, during the Holocene,  
670 *Quaternary Science Reviews*, 29, 3861-3874, <https://doi.org/10.1016/j.quascirev.2010.09.005>, 2010.

671

672 Christ, A. J., Bierman, P. R., Knutz, P. C., Corbett, L. B., Fosdick, J. C., Thomas, E. K., Cowling, O. C., Hidy, A. J.,  
673 and Caffee, M. W.: The Northwestern Greenland Ice Sheet During The Early Pleistocene Was Similar To  
674 Today, *Geophysical Research Letters*, 47, e2019GL085176, <https://doi.org/10.1029/2019GL085176>, 2020.

675

676 Christ Andrew, J., Bierman Paul, R., Schaefer Joerg, M., Dahl-Jensen, D., Steffensen Jørgen, P., Corbett Lee, B.,  
677 Peteet Dorothy, M., Thomas Elizabeth, K., Steig Eric, J., Rittenour Tammy, M., Tison, J.-L., Blard, P.-H.,  
678 Perdrial, N., Dethier David, P., Lini, A., Hidy Alan, J., Caffee Marc, W., and Southon, J.: A multimillion-year-old  
679 record of Greenland vegetation and glacial history preserved in sediment beneath 1.4 km of ice at Camp  
680 Century, *Proceedings of the National Academy of Sciences*, 118, e2021442118, 10.1073/pnas.2021442118,  
681 2021.

682

683 Cluett Allison, A. and Thomas Elizabeth, K.: Summer warmth of the past six interglacials on Greenland,  
684 Proceedings of the National Academy of Sciences, 118, e2022916118, 10.1073/pnas.2022916118, 2021.  
685  
686 Colgan, W., MacGregor, J. A., Mankoff, K. D., Haagenson, R., Rajaram, H., Martos, Y. M., Morlighem, M.,  
687 Fahnestock, M. A., and Kjeldsen, K. K.: Topographic Correction of Geothermal Heat Flux in Greenland and  
688 Antarctica, Journal of Geophysical Research: Earth Surface, 126, e2020JF005598,  
689 <https://doi.org/10.1029/2020JF005598>, 2021.  
690  
691 Dahl-Jensen, D., Albert, M. R., Aldahan, A., Azuma, N., Balslev-Clausen, D., Baumgartner, M., Berggren, A. M.,  
692 Bigler, M., Binder, T., Blunier, T., Bourgeois, J. C., Brook, E. J., Buchardt, S. L., Buizert, C., Capron, E.,  
693 Chappellaz, J., Chung, J., Clausen, H. B., Cvijanovic, I., Davies, S. M., Ditlevsen, P., Eicher, O., Fischer, H., Fisher,  
694 D. A., Fleet, L. G., Gfeller, G., Gkinis, V., Gogineni, S., Goto-Azuma, K., Grinsted, A., Gudlaugsdottir, H.,  
695 Guillevic, M., Hansen, S. B., Hansson, M., Hirabayashi, M., Hong, S., Hur, S. D., Huybrechts, P., Hvidberg, C. S.,  
696 Iizuka, Y., Jenk, T., Johnsen, S. J., Jones, T. R., Jouzel, J., Karlsson, N. B., Kawamura, K., Keegan, K., Kettner, E.,  
697 Kipfstuhl, S., Kjær, H. A., Koutnik, M., Kuramoto, T., Köhler, P., Laepple, T., Landais, A., Langen, P. L., Larsen, L.  
698 B., Leuenberger, D., Leuenberger, M., Leuschen, C., Li, J., Lipenkov, V., Martinerie, P., Maselli, O. J., Masson-  
699 Delmotte, V., McConnell, J. R., Miller, H., Mini, O., Miyamoto, A., Montagnat-Rentier, M., Mulvaney, R.,  
700 Muscheler, R., Orsi, A. J., Paden, J., Panton, C., Pattyn, F., Petit, J. R., Pol, K., Popp, T., Possnert, G., Prié, F.,  
701 Prokopiou, M., Quiquet, A., Rasmussen, S. O., Raynaud, D., Ren, J., Reutenauer, C., Ritz, C., Röckmann, T.,  
702 Rosen, J. L., Rubino, M., Rybak, O., Samyn, D., Sapart, C. J., Schilt, A., Schmidt, A. M. Z., Schwander, J.,  
703 Schüpbach, S., Seierstad, I., Severinghaus, J. P., Sheldon, S., Simonsen, S. B., Sjolte, J., Solgaard, A. M., Sowers,  
704 T., Sperlich, P., Steen-Larsen, H. C., Steffen, K., Steffensen, J. P., Steinhage, D., Stocker, T. F., Stowasser, C.,  
705 Sturevik, A. S., Sturges, W. T., Sveinbjörnsdottir, A., Svensson, A., Tison, J. L., Uetake, J., Vallelonga, P., van de  
706 Wal, R. S. W., van der Wel, G., Vaughn, B. H., Vinther, B., Waddington, E., Wegner, A., Weikusat, I., White, J.  
707 W. C., Wilhelms, F., Winstrup, M., Witrant, E., Wolff, E. W., Xiao, C., Zheng, J., and members, N. c.: Eemian  
708 interglacial reconstructed from a Greenland folded ice core, Nature, 493, 489-494, 10.1038/nature11789,  
709 2013.  
710  
711 Dawes, P. R.: The bedrock geology under the Inland Ice: the next major challenge for Greenland mapping,  
712 GEUS Bulletin, 17, 57-60, 10.34194/geusb.v17.5014, 2009.  
713  
714 de Vernal, A. and Hillaire-Marcel, C.: Natural Variability of Greenland Climate, Vegetation, and Ice Volume  
715 During the Past Million Years, Science, 320, 1622-1625, 10.1126/science.1153929, 2008.  
716

717 DeConto, R. M., Pollard, D., Alley, R. B., Velicogna, I., Gasson, E., Gomez, N., Sadai, S., Condron, A., Gilford, D.  
718 M., Ashe, E. L., Kopp, R. E., Li, D., and Dutton, A.: The Paris Climate Agreement and future sea-level rise from  
719 Antarctica, *Nature*, 593, 83-89, 10.1038/s41586-021-03427-0, 2021.  
720  
721 Domingo, D., Malmierca-Vallet, I., Sime, L., Voss, J., and Capron, E.: Using Ice Cores and Gaussian Process  
722 Emulation to Recover Changes in the Greenland Ice Sheet During the Last Interglacial, *Journal of Geophysical*  
723 *Research: Earth Surface*, 125, e2019JF005237, <https://doi.org/10.1029/2019JF005237>, 2020.  
724  
725 Dyer, B., Austermann, J., D'Andrea William, J., Creel Roger, C., Sandstrom Michael, R., Cashman, M., Rovere,  
726 A., and Raymo Maureen, E.: Sea-level trends across The Bahamas constrain peak last interglacial ice melt,  
727 *Proceedings of the National Academy of Sciences*, 118, e2026839118, 10.1073/pnas.2026839118, 2021.  
728  
729 Goelzer, H., Huybrechts, P., Loutre, M. F., and Fichefet, T.: Last Interglacial climate and sea-level evolution  
730 from a coupled ice sheet–climate model, *Clim. Past*, 12, 2195-2213, 10.5194/cp-12-2195-2016, 2016.  
731  
732 Goelzer, H., Nowicki, S., Payne, A., Larour, E., Seroussi, H., Lipscomb, W. H., Gregory, J., Abe-Ouchi, A.,  
733 Shepherd, A., Simon, E., Agosta, C., Alexander, P., Aschwanden, A., Barthel, A., Calov, R., Chambers, C., Choi,  
734 Y., Cuzzone, J., Dumas, C., Edwards, T., Felikson, D., Fettweis, X., Golledge, N. R., Greve, R., Humbert, A.,  
735 Huybrechts, P., Le clec'h, S., Lee, V., Leguy, G., Little, C., Lowry, D. P., Morlighem, M., Nias, I., Quiquet, A.,  
736 Rückamp, M., Schlegel, N. J., Slater, D. A., Smith, R. S., Straneo, F., Tarasov, L., van de Wal, R., and van den  
737 Broeke, M.: The future sea-level contribution of the Greenland ice sheet: a multi-model ensemble study of  
738 ISMIP6, *The Cryosphere*, 14, 3071-3096, 10.5194/tc-14-3071-2020, 2020.  
739  
740 Goodge, J. W. and Severinghaus, J. P.: Rapid Access Ice Drill: a new tool for exploration of the deep Antarctic  
741 ice sheets and subglacial geology, *Journal of Glaciology*, 62, 1049-1064, 10.1017/jog.2016.97, 2016.  
742 Granger, D. E., Lifton, N. A., and Willenbring, J. K.: A cosmic trip: 25 years of cosmogenic nuclides in geology,  
743 *GSA Bulletin*, 125, 1379-1402, 10.1130/B30774.1, 2013.  
744  
745 Hatfield, R. G., Reyes, A. V., Stoner, J. S., Carlson, A. E., Beard, B. L., Winsor, K., and Welke, B.: Interglacial  
746 responses of the southern Greenland ice sheet over the last 430,000 years determined using particle-size  
747 specific magnetic and isotopic tracers, *Earth and Planetary Science Letters*, 454, 225-236,  
748 <https://doi.org/10.1016/j.epsl.2016.09.014>, 2016.  
749

750 Henriksen, N., Higgins, A. K., Kalsbeek, F., and Pulvertaft, T. C. R.: Greenland from Archaean to Quaternary.  
751 Descriptive text to the 1995 Geological map of Greenland, 1:2 500 000. 2nd edition, GEUS Bulletin, 18, 1-126,  
752 10.34194/geusb.v18.4993, 2009.

753

754 Henriksen, N. and Jepsen, H. F.: Precambrian crystalline basement at the head of Victoria Fjord, North  
755 Greenland, Rapport Grønlands Geologiske Undersøgelse, 126, 11-16, 10.34194/rapggu.v126.7907, 1985.

756 Jordan, T. M., Williams, C. N., Schroeder, D. M., Martos, Y. M., Cooper, M. A., Siegert, M. J., Paden, J. D.,  
757 Huybrechts, P., and Bamber, J. L.: A constraint upon the basal water distribution and thermal state of the  
758 Greenland Ice Sheet from radar bed echoes, *The Cryosphere*, 12, 2831-2854, 10.5194/tc-12-2831-2018, 2018.

759

760 Joughin, I., Das, S. B., Flowers, G. E., Behn, M. D., Alley, R. B., King, M. A., Smith, B. E., Bamber, J. L., van den  
761 Broeke, M. R., and van Angelen, J. H.: Influence of ice-sheet geometry and supraglacial lakes on seasonal ice-  
762 flow variability, *The Cryosphere*, 7, 1185-1192, 10.5194/tc-7-1185-2013, 2013.

763

764 Keisling, B. A., Nielsen, L. T., Hvidberg, C. S., Nuterman, R., and DeConto, R. M.: Pliocene–Pleistocene  
765 megafloods as a mechanism for Greenlandic megacanyon formation, *Geology*, 48, 737-741,  
766 10.1130/G47253.1, 2020.

767

768 Keisling, B.A., Schaefer, J.M., DeConto, R.M., Briner, J.P., Young, N.E., Walcott, C., Winckler, G., Balter-  
769 Kennedy, A., Anandakrishnan, S.: Greenland ice sheet vulnerability under diverse climatic warming scenarios,  
770 *Earth ArXiv*, doi.org/10.31223/X5Q05T, 2022.

771

772 Knutz, P. C., Newton, A. M. W., Hopper, J. R., Huuse, M., Gregersen, U., Sheldon, E., and Dybkjær, K.: Eleven  
773 phases of Greenland Ice Sheet shelf-edge advance over the past 2.7 million years, *Nature Geoscience*, 12,  
774 361-368, 10.1038/s41561-019-0340-8, 2019.

775

776 Kuhl, T., Gibson, C., Johnson, J., Boeckmann, G., Moravec, E., and Slawny, K.: Agile Sub-Ice Geological (ASIG)  
777 Drill development and Pirrit Hills field project, *Annals of Glaciology*, 62, 53-66, 10.1017/aog.2020.59, 2021.

778

779 Kulesa, B., Hubbard Alun, L., Booth Adam, D., Bougamont, M., Dow Christine, F., Doyle Samuel, H.,  
780 Christoffersen, P., Lindbäck, K., Pettersson, R., Fitzpatrick Andrew, A. W., and Jones Glenn, A.: Seismic  
781 evidence for complex sedimentary control of Greenland Ice Sheet flow, *Science Advances*, 3, e1603071,  
782 10.1126/sciadv.1603071, 2017.

783

784 Li, J., Paden, J., Leuschen, C., Rodriguez-Morales, F., Hale, R. D., Arnold, E. J., Crowe, R., Gomez-Garcia, D., and  
785 Gogineni, P.: High-Altitude Radar Measurements of Ice Thickness Over the Antarctic and Greenland Ice  
786 Sheets as a Part of Operation IceBridge, *IEEE Transactions on Geoscience and Remote Sensing*, 51, 742-754,  
787 10.1109/TGRS.2012.2203822, 2013.

788

789 MacGregor, J. A., Bottke Jr, W. F., Fahnestock, M. A., Harbeck, J. P., Kjær, K. H., Paden, J. D., Stillman, D. E.,  
790 and Studinger, M.: A Possible Second Large Subglacial Impact Crater in Northwest Greenland, *Geophysical  
791 Research Letters*, 46, 1496-1504, <https://doi.org/10.1029/2018GL078126>, 2019.

792

793 MacGregor, J. A., Chu, W., Colgan, W. T., Fahnestock, M. A., Felikson, D., Karlsson, N. B., Nowicki, S. M. J., and  
794 Studinger, M.: GBaTSv2: A revised synthesis of the likely basal thermal state of the Greenland Ice Sheet, *The  
795 Cryosphere Discuss.*, 2022, 1-25, 10.5194/tc-2022-40, 2022.

796

797 MacGregor, J. A., Fahnestock, M. A., Colgan, W. T., Larsen, N. K., Kjeldsen, K. K., and Welker, J. M.: The age of  
798 surface-exposed ice along the northern margin of the Greenland Ice Sheet, *Journal of Glaciology*, 66, 667-684,  
799 10.1017/jog.2020.62, 2020.

800

801 McNabb, R. W., Hock, R., O'Neel, S., Rasmussen, L. A., Ahn, Y., Braun, M., Conway, H., Herreid, S., Joughin, I.,  
802 Pfeffer, W. T., Smith, B. E., and Truffer, M.: Using surface velocities to calculate ice thickness and bed  
803 topography: a case study at Columbia Glacier, Alaska, USA, *Journal of Glaciology*, 58, 1151-1164,  
804 10.3189/2012JogG11J249, 2012.

805

806 Morlighem, M., Rignot, E., Mougnot, J., Seroussi, H., and Larour, E.: Deeply incised submarine glacial valleys  
807 beneath the Greenland ice sheet, *Nature Geoscience*, 7, 418-422, 10.1038/ngeo2167, 2014.

808

809 Morlighem, M., Rignot, E., Seroussi, H., Larour, E., Ben Dhia, H., and Aubry, D.: A mass conservation approach  
810 for mapping glacier ice thickness, *Geophysical Research Letters*, 38, <https://doi.org/10.1029/2011GL048659>,  
811 2011.

812

813 Morlighem, M., Williams, C. N., Rignot, E., An, L., Arndt, J. E., Bamber, J. L., Catania, G., Chauché, N.,  
814 Dowdeswell, J. A., Dorschel, B., Fenty, I., Hogan, K., Howat, I., Hubbard, A., Jakobsson, M., Jordan, T. M.,  
815 Kjeldsen, K. K., Millan, R., Mayer, L., Mougnot, J., Noël, B. P. Y., O'Cofaigh, C., Palmer, S., Rysgaard, S.,  
816 Seroussi, H., Siegert, M. J., Slabon, P., Straneo, F., van den Broeke, M. R., Weinrebe, W., Wood, M., and  
817 Zinglensen, K. B.: BedMachine v3: Complete Bed Topography and Ocean Bathymetry Mapping of Greenland

818 From Multibeam Echo Sounding Combined With Mass Conservation, *Geophysical Research Letters*, 44,  
819 11,051-011,061, <https://doi.org/10.1002/2017GL074954>, 2017.

820

821 Nishiizumi, K., Finkel, R. C., Ponganis, K. V., Graf, T., Kohl, C. P., and Marti, K.: In situ produced cosmogenic  
822 nuclides in GISP2 rock core from Greenland summit, *Eos*, 77, F428, 1996.

823

824 Paxman, G. J. G., Austermann, J., and Tinto, K. J.: A fault-bounded palaeo-lake basin preserved beneath the  
825 Greenland Ice Sheet, *Earth and Planetary Science Letters*, 553, 116647,  
826 <https://doi.org/10.1016/j.epsl.2020.116647>, 2021.

827

828 Pedersen, M., Weng, W. L., Keulen, N., and Kokfelt, T. F.: A new seamless digital 1:500 000 scale geological  
829 map of Greenland, *GEUS Bulletin*, 28, 65-68, 10.34194/geusb.v28.4727, 2013.

830

831 Plach, A., Nisancioglu, K. H., Le clec'h, S., Born, A., Langebroek, P. M., Guo, C., Imhof, M., and Stocker, T. F.:  
832 Eemian Greenland SMB strongly sensitive to model choice, *Clim. Past*, 14, 1463-1485, 10.5194/cp-14-1463-  
833 2018, 2018.

834

835 Poinar, K. and Andrews, L. C.: Challenges in predicting Greenland supraglacial lake drainages at the regional  
836 scale, *The Cryosphere*, 15, 1455-1483, 10.5194/tc-15-1455-2021, 2021.

837

838 Reyes, A. V., Carlson, A. E., Beard, B. L., Hatfield, R. G., Stoner, J. S., Winsor, K., Welke, B., and Ullman, D. J.:  
839 South Greenland ice-sheet collapse during Marine Isotope Stage 11, *Nature*, 510, 525-528,  
840 10.1038/nature13456, 2014.

841

842 Robinson, A., Alvarez-Solas, J., Calov, R., Ganopolski, A., and Montoya, M.: MIS-11 duration key to  
843 disappearance of the Greenland ice sheet, *Nature Communications*, 8, 16008, 10.1038/ncomms16008, 2017.

844

845 Rogozhina, I., Petrunin, A. G., Vaughan, A. P. M., Steinberger, B., Johnson, J. V., Kaban, M. K., Calov, R.,  
846 Rickers, F., Thomas, M., and Koulakov, I.: Melting at the base of the Greenland ice sheet explained by Iceland  
847 hotspot history, *Nature Geoscience*, 9, 366-369, 10.1038/ngeo2689, 2016.

848

849 Scambos, T. A., Bell, R. E., Alley, R. B., Anandakrishnan, S., Bromwich, D. H., Brunt, K., Christianson, K., Creyts,  
850 T., Das, S. B., DeConto, R., Dutrieux, P., Fricker, H. A., Holland, D., MacGregor, J., Medley, B., Nicolas, J. P.,  
851 Pollard, D., Siegfried, M. R., Smith, A. M., Steig, E. J., Trusel, L. D., Vaughan, D. G., and Yager, P. L.: How much,



852 how fast?: A science review and outlook for research on the instability of Antarctica's Thwaites Glacier in the  
853 21st century, *Global and Planetary Change*, 153, 16-34, <https://doi.org/10.1016/j.gloplacha.2017.04.008>,  
854 2017.

855

856 Schaefer, J. M., Finkel, R. C., Balco, G., Alley, R. B., Caffee, M. W., Briner, J. P., Young, N. E., Gow, A. J., and  
857 Schwartz, R.: Greenland was nearly ice-free for extended periods during the Pleistocene, *Nature*, 540, 252-  
858 255, 10.1038/nature20146, 2016.

859

860 Shepherd, A., Ivins, E., Rignot, E., Smith, B., van den Broeke, M., Velicogna, I., Whitehouse, P., Briggs, K.,  
861 Joughin, I., Krinner, G., Nowicki, S., Payne, T., Scambos, T., Schlegel, N., A. G., Agosta, C., Ahlstrøm, A.,  
862 Babonis, G., Barletta, V., Blazquez, A., Bonin, J., Csatho, B., Cullather, R., Felikson, D., Fettweis, X., Forsberg,  
863 R., Gallee, H., Gardner, A., Gilbert, L., Groh, A., Gunter, B., Hanna, E., Harig, C., Helm, V., Horvath, A.,  
864 Horwath, M., Khan, S., Kjeldsen, K. K., Konrad, H., Langen, P., Lecavalier, B., Loomis, B., Luthcke, S., McMillan,  
865 M., Melini, D., Mernild, S., Mohajerani, Y., Moore, P., Mougnot, J., Moyano, G., Muir, A., Nagler, T., Nield, G.,  
866 Nilsson, J., Noel, B., Ootaka, I., Pattle, M. E., Peltier, W. R., Pie, N., Rietbroek, R., Rott, H., Sandberg-  
867 Sørensen, L., Sasgen, I., Save, H., Scheuchl, B., Schrama, E., Schröder, L., Seo, K.-W., Simonsen, S., Slater, T.,  
868 Spada, G., Sutterley, T., Talpe, M., Tarasov, L., van de Berg, W. J., van der Wal, W., van Wessem, M.,  
869 Vishwakarma, B. D., Wiese, D., Wouters, B., and The, I. t.: Mass balance of the Antarctic Ice Sheet from 1992  
870 to 2017, *Nature*, 558, 219-222, 10.1038/s41586-018-0179-y, 2018.

871

872 Shepherd, A., Ivins, E., Rignot, E., Smith, B., van den Broeke, M., Velicogna, I., Whitehouse, P., Briggs, K.,  
873 Joughin, I., Krinner, G., Nowicki, S., Payne, T., Scambos, T., Schlegel, N., A. G., Agosta, C., Ahlstrøm, A.,  
874 Babonis, G., Barletta, V. R., Bjørk, A. A., Blazquez, A., Bonin, J., Colgan, W., Csatho, B., Cullather, R., Engdahl,  
875 M. E., Felikson, D., Fettweis, X., Forsberg, R., Hogg, A. E., Gallee, H., Gardner, A., Gilbert, L., Gourmelen, N.,  
876 Groh, A., Gunter, B., Hanna, E., Harig, C., Helm, V., Horvath, A., Horwath, M., Khan, S., Kjeldsen, K. K., Konrad,  
877 H., Langen, P. L., Lecavalier, B., Loomis, B., Luthcke, S., McMillan, M., Melini, D., Mernild, S., Mohajerani, Y.,  
878 Moore, P., Mottram, R., Mougnot, J., Moyano, G., Muir, A., Nagler, T., Nield, G., Nilsson, J., Noël, B., Ootaka,  
879 I., Pattle, M. E., Peltier, W. R., Pie, N., Rietbroek, R., Rott, H., Sandberg Sørensen, L., Sasgen, I., Save, H.,  
880 Scheuchl, B., Schrama, E., Schröder, L., Seo, K.-W., Simonsen, S. B., Slater, T., Spada, G., Sutterley, T., Talpe,  
881 M., Tarasov, L., van de Berg, W. J., van der Wal, W., van Wessem, M., Vishwakarma, B. D., Wiese, D., Wilton,  
882 D., Wagner, T., Wouters, B., Wuite, J., and The, I. T.: Mass balance of the Greenland Ice Sheet from 1992 to  
883 2018, *Nature*, 579, 233-239, 10.1038/s41586-019-1855-2, 2020.

884

885 Sommers, A. N., Otto-Bliesner, B. L., Lipscomb, W. H., Lofverstrom, M., Shafer, S. L., Bartlein, P. J., Brady, E. C.,  
886 Kluzek, E., Leguy, G., Thayer-Calder, K., and Tomas, R. A.: Retreat and Regrowth of the Greenland Ice Sheet  
887 During the Last Interglacial as Simulated by the CESM2-CISM2 Coupled Climate–Ice Sheet Model,  
888 *Paleoceanography and Paleoclimatology*, 36, e2021PA004272, <https://doi.org/10.1029/2021PA004272>, 2021.  
889  
890 Spector, P., Stone, J., Cowdery, S. G., Hall, B., Conway, H., and Bromley, G.: Rapid early-Holocene deglaciation  
891 in the Ross Sea, Antarctica, *Geophysical Research Letters*, 44, 7817-7825,  
892 <https://doi.org/10.1002/2017GL074216>, 2017.  
893  
894 Spector, P., Stone, J., Pollard, D., Hillebrand, T., Lewis, C., and Gombiner, J.: West Antarctic sites for subglacial  
895 drilling to test for past ice-sheet collapse, *The Cryosphere*, 12, 2741-2757, [10.5194/tc-12-2741-2018](https://doi.org/10.5194/tc-12-2741-2018), 2018.  
896  
897 Sugden, D. E.: Glacial Erosion by the Laurentide Ice Sheet, *Journal of Glaciology*, 20, 367-391,  
898 [10.3189/S002214300013915](https://doi.org/10.3189/S002214300013915), 1978.  
899  
900 Timoney, R., Worrall, K., Firstbrook, D., Harkness, P., Rix, J., Ashurst, D., Mulvaney, R., and Bentley, M. J.: A  
901 low resource subglacial bedrock sampler: The percussive rapid access isotope drill (P-RAID), *Cold Regions  
902 Science and Technology*, 177, 103113, <https://doi.org/10.1016/j.coldregions.2020.103113>, 2020.  
903  
904 Willerslev, E., Cappellini, E., Boomsma, W., Nielsen, R., Hebsgaard Martin, B., Brand Tina, B., Hofreiter, M.,  
905 Bunce, M., Poinar Hendrik, N., Dahl-Jensen, D., Johnsen, S., Steffensen Jørgen, P., Bennike, O., Schwenninger,  
906 J.-L., Nathan, R., Armitage, S., de Hoog, C.-J., Alfimov, V., Christl, M., Beer, J., Muscheler, R., Barker, J., Sharp,  
907 M., Penkman Kirsty, E. H., Haile, J., Taberlet, P., Gilbert, M. T. P., Casoli, A., Campani, E., and Collins Matthew,  
908 J.: Ancient Biomolecules from Deep Ice Cores Reveal a Forested Southern Greenland, *Science*, 317, 111-114,  
909 [10.1126/science.1141758](https://doi.org/10.1126/science.1141758), 2007.  
910  
911 Yau, A. M., Bender, M. L., Blunier, T., and Jouzel, J.: Setting a chronology for the basal ice at Dye-3 and GRIP:  
912 Implications for the long-term stability of the Greenland Ice Sheet, *Earth and Planetary Science Letters*, 451,  
913 1-9, <https://doi.org/10.1016/j.epsl.2016.06.053>, 2016.  
914  
915 Yau Audrey, M., Bender Michael, L., Robinson, A., and Brook Edward, J.: Reconstructing the last interglacial at  
916 Summit, Greenland: Insights from GISP2, *Proceedings of the National Academy of Sciences*, 113, 9710-9715,  
917 [10.1073/pnas.1524766113](https://doi.org/10.1073/pnas.1524766113), 2016.  
918

919 Young, N. E., Lesnek, A. J., Cuzzone, J. K., Briner, J. P., Badgeley, J. A., Balter-Kennedy, A., Graham, B. L.,  
920 Cluett, A., Lamp, J. L., Schwartz, R., Tuna, T., Bard, E., Caffee, M. W., Zimmerman, S. R. H., and Schaefer, J. M.:  
921 In situ cosmogenic  $^{10}\text{Be}$ – $^{14}\text{C}$ – $^{26}\text{Al}$  measurements from recently deglaciated bedrock as a new tool to  
922 decipher changes in Greenland Ice Sheet size, *Climate of the Past*, 17, 419-450, [http://dx.doi.org/10.5194/cp-](http://dx.doi.org/10.5194/cp-17-419-2021)  
923 17-419-2021, 2021.